EMSA—A nuclear extract of MIN6 cells was prepared as described previously (16). Then 5 μg of the nuclear extract was incubated with ^{32}P-radiolabeled oligonucleotides containing the HNF4α or HNF1α binding sequence in a mixture containing 10 mM Tris-HCl (pH 7.5), 1% Ficoll, 70 mM KCl, 30 mg/ml BSA, 4.8% glycerol, and 100 μg/ml poly(dI-dC). Next, the DNA-protein complexes were resolved on 4% polyacrylamide gel in 0.5× Tris-borate-EDTA buffer at 120 V for 2 h, after which the dried gel was exposed to a phosphorimaging screen and analyzed with a BAS 2000 (Fuji Film). The oligonucleotide sequences were as follows: wild-type HNF4α binding site (5′-GGCCGGAGTGAACTTTGGCCTGGGGTGATA-3′); mutant HNF4α binding site (5′-GGCCGGAGTGAATGGGAGCCTGGGGTGATA-3′); wild-type HNF1α binding site (5′-CCCCGTCACTGATTAACCAGCCCTGTTGGA-3′); and mutant HNF1α binding site (5′-CCCCGTCACTGACCGGCCAGCCCTGTTGGA-3′). An anti-HNF1 antibody (H205, sc-8986) was used for the supershift assay.

Chromatin Immunoprecipitation—MIN6 cells were fixed in DMEM containing 1% formaldehyde for 10 min at room temperature, and then cross-linking was quenched by placing the cells in 200 mM glycine for 5 min at room temperature. The cells were incubated in Nonidet P-40 buffer (10 mM Tris-HCl (pH 8.0), 10 mM NaCl, 0.5% Nonidet P-40) for 5 min at room temperature and then lysed in SDS lysis buffer (50 mM Tris-HCl (pH 8.0), 1% SDS, 10 mM EDTA) followed by 5-fold dilution in ChIP dilution buffer (50 mM Tris-HCl (pH 8.0), 167 mM NaCl, 1.1% Triton X-100, and 0.11% sodium deoxycholate). Sonication was performed with a Sonifier 150 (Branson). Soluble sheared chromatin (20 μg) was incubated overnight at 4 °C with magnetic beads (Invitrogen Dynabeads protein G) bound to 2 μg of anti-HNF4α antibody (Santa Cruz Biotechnology sc-6556), anti-RNA polymerase II monoclonal antibody (Active Motif), or control IgG (Cell Signaling Technology antibody 2729) followed by sequential washing with low salt radioimmunoprecipitation assay buffer (50 mM Tris-HCl (pH 8.0), 150 mM NaCl, 1 mM EDTA, 0.1% SDS, 1% Triton X-100, and 0.1% sodium deoxycholate), high salt radioimmunoprecipitation assay buffer (50 mM Tris-HCl (pH 8.0), 500 mM NaCl, 1 mM EDTA, 0.1% SDS, 1% Triton X-100, and 0.1% sodium deoxycholate), wash buffer (50 mM Hepes-KOH (pH 7.5), 500 mM LiCl, 1 mM EDTA, 1% Nonidet P-40, and 0.7% sodium deoxycholate), and Tris-EDTA. Then immune complexes were eluted from the magnetic beads by incubation with ChIP direct elution buffer (50 mM Tris-HCl (pH 8.0), 10 mM EDTA, and 1% SDS) for 20 min at 65 °C. For reverse cross-linking, the eluate was incubated overnight at 65 °C, and then DNA fragments were purified by using a PCR purification kit (Qiagen). PCR was performed to identify Anks4b promoter fragments in the immunoprecipitated DNA using a pair of primers (5′-TTCACCACACTCATGACACACC-3′ and 5′-AGGTAGGAGTCTTTGTCTAGGC-3′).

GST Pulldown Assay—Mouse Anks4b cDNA was amplified by PCR using a pair of primers (5′-CGGATCCCCATGTCTACCCGCTATCACCAA-3′ and 5′-CGGATCCTTAGAGGCTGGTGTCAACCAACT-3′) and was subcloned into the pGEX4T2 vector (GE Healthcare). Anks4b deletion mutants (N-Anks4b (amino acid residues 1–126), M-Anks4b (amino acid residues 127–345), and C-Anks4b (amino acid residues 346–423)) were also generated by PCR and subcloned into the pGEX4T3 vector (GE Healthcare). GST-Anks4b proteins were expressed in *E. coli* BL21 (DE3) and purified with glutathione-Sepharose 4B beads (GE Healthcare). GST or GST fusion proteins (20 μg) immobilized on glutathione-Sepharose beads were incubated with 500 μg of mouse liver lysate. After binding overnight at 4 °C, the beads were washed with lysis buffer containing 10 mM Tris-HCl (pH 7.4), 150 mM NaCl, 1% Nonidet P-40, 1 mM EDTA, 10 mM NaF, 10 mM $Na_4P_2O_7$, 1 mM PMSF, and protease inhibitor mixture (Nacalai Tesque). Then the bound proteins were separated by SDS-PAGE.

Proteomic Identification of Anks4b-interacting Proteins—Silver-stained gels were subjected to in-gel digestion followed by extraction of peptides and proteomic analysis by LC-MS/MS. Gel digestion and peptide extraction were performed as reported previously (17). The peptide samples thus obtained were analyzed in an ESI-Q-TOF tandem mass spectrometer (6510; Agilent) with an HPLC chip-MS system, consisting of a nano pump (G2226; Agilent) with a four-channel microvacuum degasser (G1379B; Agilent), a microfluidic chip cube (G4240; Agilent), a capillary pump (G1376A; Agilent) with degasser (G1379B; Agilent), and an autosampler with thermostat (G1377A; Agilent). All modules were controlled by MassHunter software (version B.02.00; Agilent). A microfluidic reverse-phase-HPLC chip (Zorbax 300SB-C18; 5-μm particle size, 75-mm inner diameter, and 43 mm in length) was used for separation of peptides. The nano pump was employed to generate gradient nano flow at 600 nl/min, with the mobile phase being 0.1% formic acid in MS-grade water (solvent A) and 0.1% formic acid in acetonitrile (solvent B). The gradient was 5–75% solvent B over 9 min. A capillary pump was used to load samples with a mobile phase of 0.1% formic acid at 4 μl/min. The Agilent ESI-Q-TOF was operated in the positive ionization mode (ESI+), with an ionization voltage of 1,850 V and a fragmentor voltage of 175 V at 300 °C. Fragmentation of protonated molecular ions was conducted in the auto-MS/MS mode, starting with a collision energy voltage of 3 V that was increased by 3.7 V per 100 Da. The selected m/z ranges were 300–2,400 Da in the MS mode and 59–3,000 Da in the MS/MS mode. The data output consisted of one full mass spectrum (with three fragmentation patterns per spectrum) every 250 ms. The three highest peaks of each MS spectrum were selected for fragmentation. Mass lists were created in the form of Mascot generic files and were used as the input for Mascot MS/MS ion searches of the National Center for Biotechnology Information nonredundant (NCBI nr) database using the Matrix Science Web server Mascot version 2.2. Default search parameters were as follows: enzyme, trypsin; maximum missed cleavage, 1; variable modifications, carbamidomethyl (Cys); peptide tolerance, ± 1.2 Da; MS/MS tolerance, ± 0.6 Da; peptide charge, 2+ and 3+; instrument, ESI-Q-TOF. For positive identification, the result of $(-10 \times \log(p))$ could not exceed the significance threshold ($p < 0.05$).

Immunoprecipitation—Mouse Anks4b cDNA was amplified by PCR using a pair of primers (5′-CGGATCCCCATGTCTACCCGCTATCACCAA-3′ and 5′-CGGATCCTTAGAGGCTGGTGTCAACCAACT-3′) and was subcloned in-frame

into the pcDNA3-HA and pcDNA3-FLAG expression vectors. The GRP78 expression vector (pCMV-BiP-Myc-KDEL-wt) was a gift from Dr. Ron Prywes (Addgene plasmid 27164). After transfection into COS-7 cells, the cells were lysed in immunoprecipitation buffer (20 mM Tris-HCl (pH 7.4), 175 mM NaCl, 2.5 mM $MgCl_2$, 0.05% Nonidet P-40, 1 mM PMSF, and protease inhibitor mixture (Nacalai Tesque)) and incubated on ice for 30 min. Then 700 μg of cell lysate and FLAG tag antibody beads (Wako) were mixed and stirred at 4 °C for 18 h. After washing with immunoprecipitation buffer, proteins were eluted by using DYKDDDDK peptide (Wako). A sample of the eluate and 2% of the cell lysate (from before processing) were subjected to Western blotting analysis.

Immunocytochemistry—Both the pcDNA3-HA-Anks4b and the pCMV-BiP-Myc-KDEL-wt vectors were transfected into HeLa, COS-7, and MIN6 cells with X-treme GENE (Roche Diagnostics) for 24 h. Then the cells were fixed in 10% neutralized formalin and permeabilized with 0.1% Triton X-100, 3% BSA/PBS. Monoclonal rat anti-HA antibody (1:400) (clone 3F10, Roche Applied Science) and mouse anti-c-Myc antibody (1:400) (Wako) were used as the primary antibodies, whereas Alexa Fluor 568 goat anti-rat IgG (Invitrogen) and Alexa Fluor 488 goat anti-mouse IgG (Invitrogen) were used as the secondary antibodies. Immunofluorescence was detected under a laser scanning confocal microscope (FV-1000, Olympus, Tokyo, Japan).

Retrovirus Infection—Mouse Anks4b and human HNF4α7 cDNAs were subcloned into the pMXs-puro retrovirus vector for overexpression (18). Specific shRNA sequences for mouse HNF4α (5′-CCAAGAGCTGCAGATTGAT-3′) and Anks4b (5′-GAAGAAGACTCATTTCCAA-3′) were designed using the Clontech RNAi target sequence selector. Oligonucleotides encoding shRNA were synthesized and cloned into the pSIREN-RetroQ retroviral shRNA expression vector (Clontech). Then the pMXs-Anks4b, pMXs-HNF4α7, and empty pMXs vectors were transfected into Plat-E cells using FuGENE6 (Roche Applied Science, Mannheim, Germany). For knockdown experiments, transfection was done with pSIREN-RetroQ-Anks4b, pSIREN-RetroQ-HNF4α, and the negative control pSIREN-RetroQ vector. MIN6 cells were infected with the retroviruses and selected by incubation with puromycin (5 μg/ml) (12).

Flow Cytometric Analysis—An annexin V-FITC apoptosis detection kit (BioVision Research Products, Mountain View, CA) was used for the apoptosis assay according to the manufacturer's instructions. MIN6 cells were cultured in DMEM for 30 h with or without 1 μM thapsigargin (Nacalai Tesque). After incubation in trypsin/EDTA for 10 min at 37 °C, cells were centrifuged at 6,000 rpm for 10 min. The pellet was resuspended in 1×resuspension buffer, and the cells were stained with annexin V-FITC antibody. After incubation for 5 min at room temperature in the dark, stained cells were analyzed using a FACSCalibur (BD Biosciences) and FlowJo software (Tomy Digital Biology, Tokyo, Japan).

Statistical Analysis—Statistical analyses were performed using Statview J-5.0 software (SAS Institute, Cary, NC). The significance of differences was assessed with the unpaired *t* test, and $p < 0.05$ was considered to indicate statistical significance.

RESULTS

Anks4b Is a Novel Target of HNF4α—To identify target genes of HNF4α in pancreatic β-cells, DNA microarray analysis was performed using islets from βHNF4α KO mice and control mice. Body weight and blood glucose levels were similar for these two strains of mice (body weight was 32.7 ± 1.7 g ($n = 5$) *versus* 34.1 ± 1.9 g ($n = 5$) and random blood glucose was 128 ± 27 mg/dl ($n = 5$) *versus* 114 ± 24 mg/dl ($n = 5$) for βHNF4α KO *versus* control mice). Microarray analysis identified 56 up-regulated genes (signal log ratio ≥2) and 100 down-regulated genes (signal log ratio ≤−1.5) in βHNF4α KO islets (supplemental Table 2). Expression of the majority of the genes known to be involved in glucose metabolism was unchanged. To validate these results, expression of mRNA for genes randomly chosen from both the down-regulated and the up-regulated groups was assessed by quantitative real-time PCR in an independent group of 12-week-old male mice. As a result, differential expression of most genes was confirmed (Fig. 1*A* and supplemental Fig. 1). Gupta *et al.* (19) reported that ST5, a regulator of ERK activation, is a direct target of HNF4α in β-cells. Expression of ST5 mRNA was reduced by 24.6% in βHNF4α KO islets (supplemental Fig. 2).

Next, we performed a computational scan of the HNF4α binding motif in the down-regulated genes. This identified 22 high affinity HNF4α binding sequences in the mouse promoter. In 3 out of 22 genes, the HNF4 motif was also conserved in the corresponding human genome. These three genes encoded *Anks4b*, guanylate cyclase 2c (*Gucy2c*), and peroxisome proliferator-activated receptor γ coactivator-1α (*Ppargc1a*). Quantitative real-time PCR analysis confirmed a significant decrease of Anks4b expression in the islets of 12-week-old βHNF4α KO mice (17.3% of the control level, $p < 0.01$) (Fig. 1*B*). In contrast, the reduction of Gucy2c mRNA expression was marginal (21.7% of the control level, $p = 0.06$), and *Ppargc1a* mRNA levels were unchanged. The difference of sex and age of mice or different detection systems might have contributed to the different results. To elucidate the direct effect of HNF4α on the expression of these three genes, we established MIN6 β-cells that stably expressed HNF4α-specific shRNA (HNF4α KD-MIN6) by retroviral infection. Suppression of endogenous HNF4α was confirmed at both the mRNA and the protein levels (Fig. 1*C*). Decreased expression of *Anks4b*, *Gucy2c*, and *Ppargc1a* was found in HNF4α KD-MIN6 cells (Fig. 1*D*). Because *Anks4b* gene expression was most markedly decreased in both βHNF4α KO islets and HNF4α KD-MIN6 cells (35.2% of the control level, $p < 0.001$), we focused on Anks4b for further investigation.

Screening of the promoter region of the mouse Anks4b gene by using a genomic databank revealed an HNF4α binding site (nucleotides −108 to −120 relative to the translation start codon when A is designated as +1). We cloned a 190-bp promoter region upstream of a luciferase reporter gene and co-expressed it with the HNF4α expression vector in HEK293 cells. Induction of HNF4α7 (an isoform expressed in pancreatic β-cells (4)) increased Anks4b promoter activity in a concentration-dependent manner (Fig. 2*A*), whereas overexpression of the HNF4α mutant lacking AF-2 had no effect (Fig. 2*B*). When

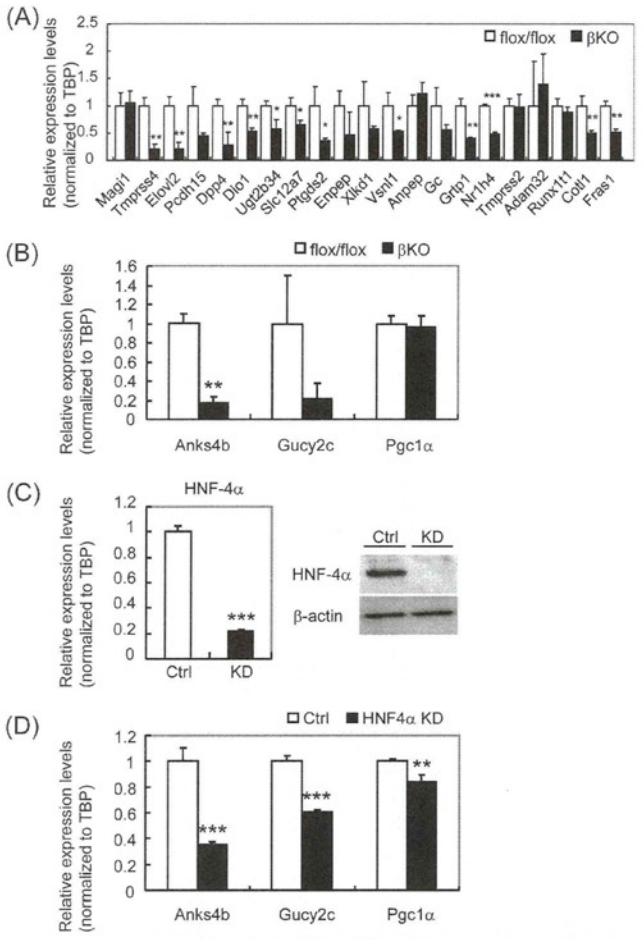

FIGURE 1. **Gene expression in the islets of βHNF4α KO mice and HNF4α knockdown MIN6 cells.** *A*, quantitative RT-PCR analysis of genes randomly chosen from those in supplemental Table 1 using flox/flox control (*white bar*) and βHNF4α KO islets (*black bar*, male, 12 week, $n = 4$). Expression of each gene was normalized for that of TATA-binding protein (*TBP*). *B*, expression of *Anks4b*, *Gucy2c*, and *Ppargc1a* in βHNF4α KO islets. Decreased expression of Anks4b was confirmed by quantitative RT-PCR. *C*, HNF4α mRNA (*left*) and HNF4α protein (*right*) in control (*Ctrl*, *white bar*) and HNF4α knockdown MIN6 cells (*KD*, *black bar*) were evaluated by quantitative PCR ($n = 4$) and Western blotting, respectively. β-Actin was used as the loading control. *D*, expression of *Anks4b*, *Gucy2c*, and *Ppargc1a* was significantly decreased in HNF4α KD-MIN6 cells. The mean ± S.D. for each group is shown (*, $p < 0.05$, **, $p < 0.01$, ***, $p < 0.001$).

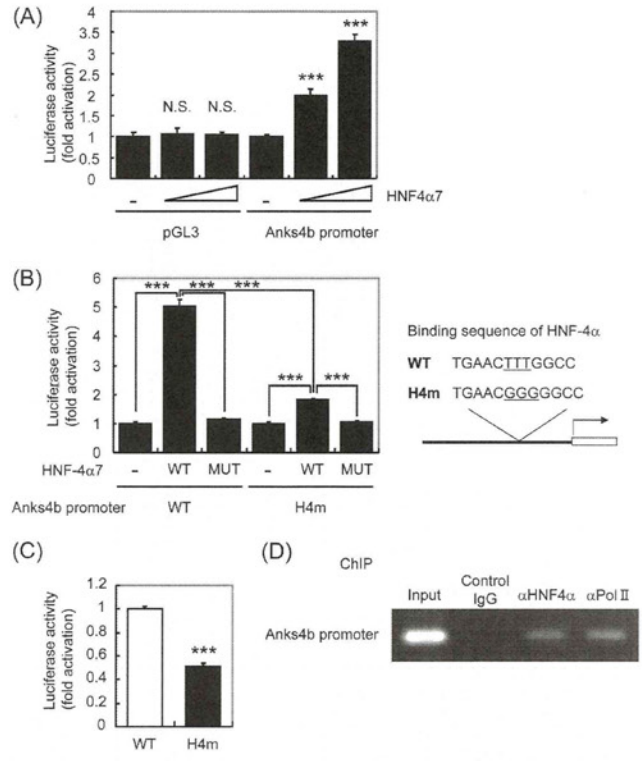

FIGURE 2. **Transcriptional regulation of Anks4b by HNF4α.** *A*, HEK293 cells were cotransfected with the pcDNA3-HNF4α7 expression vector (0–75 ng), as well as 50 ng of pGL3 basic or pGL3-Anks4b reporter and 25 ng of pRL-TK. *B*, HEK293 cells were cotransfected with 50 ng of pcDNA3-wild-type-HNF4α7 (WT) or pcDNA3-mutant (MUT) HNF4α7, as well as 50 ng of pGL3-Anks4b reporter (WT and MUT) and 25 ng of pRL-TK. *C*, MIN6 cells were transfected with pGL3-Anks4b reporter (WT and MUT) and 25 ng of pRL-TK. The mean ± S.D. for each group ($n = 3$) is shown (***, $p < 0.001$). *N.S.*, not significant. *D*, chromatin immunoprecipitation assay with MIN6 cells. Interaction of HNF4α with the promoter of Anks4b was observed. *αPol II*, RNA polymerase II antibody.

the putative HNF4α binding site in the Anks4b promoter was subjected to mutation (H4m), transcriptional activation by HNF4α7 was significantly reduced by 64.0% ($p < 0.001$) (Fig. 2*B*). Disruption of the HNF4α binding site was also associated with a 48.5% reduction of promoter activity in MIN6 cells ($p < 0.001$) (Fig. 2*C*). To assess the binding of HNF4α to the Anks4b promoter, a chromatin immunoprecipitation (ChIP) assay was performed using MIN6 cells. This assay revealed binding of HNF4α to the Anks4b promoter of MIN6 cells (Fig. 2*D*). Specific binding of HNF4α to the putative binding site was also demonstrated by the electrophoretic mobility shift assay (EMSA) (supplemental Fig. 3). Thus, both *in vivo* and *in vitro* data indicated that Anks4b is a direct target of HNF4α in β-cells.

HNF4α and HNF1α Synergistically Activate Transcription of Anks4b—HNF1α is a homeodomain-containing transcription factor that is also expressed in the liver, kidney, intestine, and pancreas (20). Mutation of the *HNF1A* gene causes another type of MODY known as MODY3 (21). In addition to the binding site for HNF4α, we also found an HNF1α binding consensus sequence in the Anks4b promoter (Fig. 3*A*). Therefore, we examined the role of HNF1α in Anks4b gene transcription. First, binding of HNF1α to the Anks4b gene was examined by EMSA with MIN6 nuclear extracts and a probe corresponding to the HNF1α binding site (Fig. 3*B*). The probe shifted after the addition of nuclear extracts (*lane 2*), and its binding was blocked by the addition of a 30-fold excess of unlabeled oligonucleotide (*lane 3*). Specificity of HNF1α binding was assessed by supershifting the DNA-HNF1α complex using HNF1α antibody (*lane 5*), indicating that HNF1α also binds directly to the Anks4b promoter. To examine the influence of HNF1α on Anks4b gene expression, we next performed a reporter gene assay. WT-HNF1α caused a dose-dependent increase of Anks4b promoter activity (Fig. 3*C*). Interestingly, Anks4b mRNA expression was decreased in HNF1α KO islets according to the results of DNA microarray analysis (22). Taken together, these results suggested that Anks4b is a target of

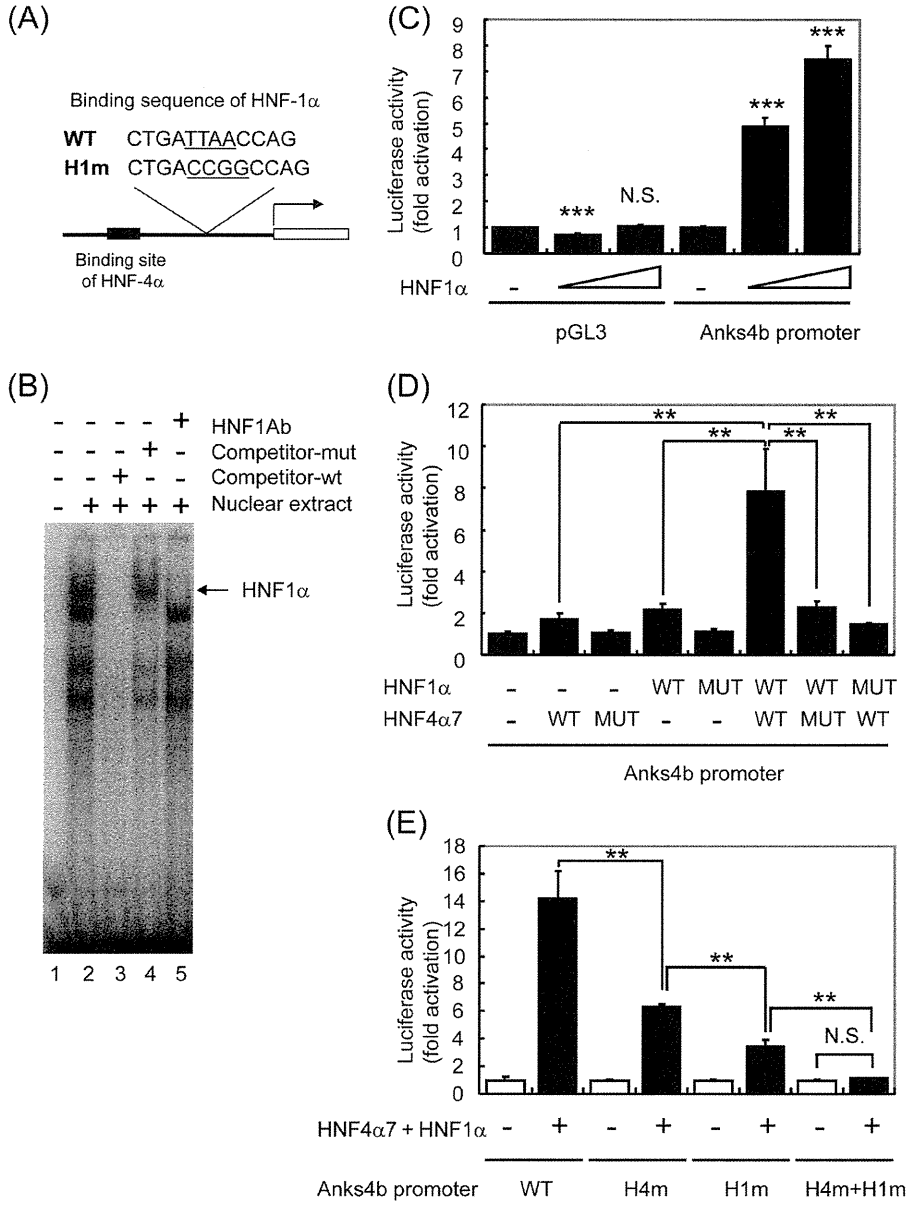

FIGURE 3. **Synergistic activation of Anks4b transcription by HNF4α and HNF1α.** *A*, DNA sequences of the promoter region of the mouse and human Anks4b genes. The putative HNF4α and HNF1α binding sites are shown. *B*, EMSA analysis of the HNF1α binding site in the Anks4b gene. DNA binding was tested using nuclear extracts from MIN6 cells. *C*, HEK293 cells were cotransfected with the pcDNA3.1-HNF1α expression vector (0–75 ng), as well as 50 ng of pGL3 basic or pGL3-Anks4b reporter and 25 ng of pRL-TK. *D*, HEK293 cells were cotransfected with 10 ng of pcDNA3.1-HNF1α (WT or MUT) and 10 ng of pcDNA3-HNF4α7 (WT or MUT), as well as 50 ng of pGL3-Anks4b reporter and 5 ng of pRL-TK. *E*, HEK293 cells were cotransfected with pcDNA3.1-HNF1α and pcDNA3-HNF4α7 as well as 50 ng of pGL3-Anks4b reporter (WT or MUT). *H4m*, mutation of the HNF4α binding site; *H1m*, mutation of the HNF1α binding site. *H4m+H1m*, mutation of both binding sites. The mean ± S.D. for each group ($n = 3$) is shown (**, $p < 0.01$, ***, $p < 0.001$). *N.S.*, not significant.

HNF1α as well as HNF4α. Because it has been reported that HNF4α and HNF1α cooperatively activate target genes that have binding sites for both HNFs in the promoter region (23, 24), we examined the influence on Anks4b gene expression of interaction between HNF4α and HNF1α. When an Anks4b reporter construct was cotransfected into HEK293 cells with 10 ng of HNF1α or HNF4α expression plasmid, the reporter gene was activated by 2.2- and 1.7-fold, respectively (Fig. 3*D*). In contrast, there was a dramatic increase of promoter activity (7.9-fold) when both constructs were cotransfected simultaneously (Fig. 3*D*). Mutation of either HNF1α or HNF4α markedly suppressed this response (Fig. 3*D*). Synergistic activation of Anks4b promoter activity was significantly suppressed by disruption of either the HNF4α binding site (H4m) or the HNF1α binding site (H1m), and activation was completely abolished by both H4m and H1m (Fig. 3*E*). Taken together, these results indicate that Anks4b promoter activity is synergistically regulated by both HNF4α and HNF1α.

Anks4b Interacts with GRP78 Both in Vitro and in Vivo—Anks4b is a scaffold protein with three ankyrin repeats and a sterile α motif domain that was identified as harmonin-interacting protein (25), although its function is completely

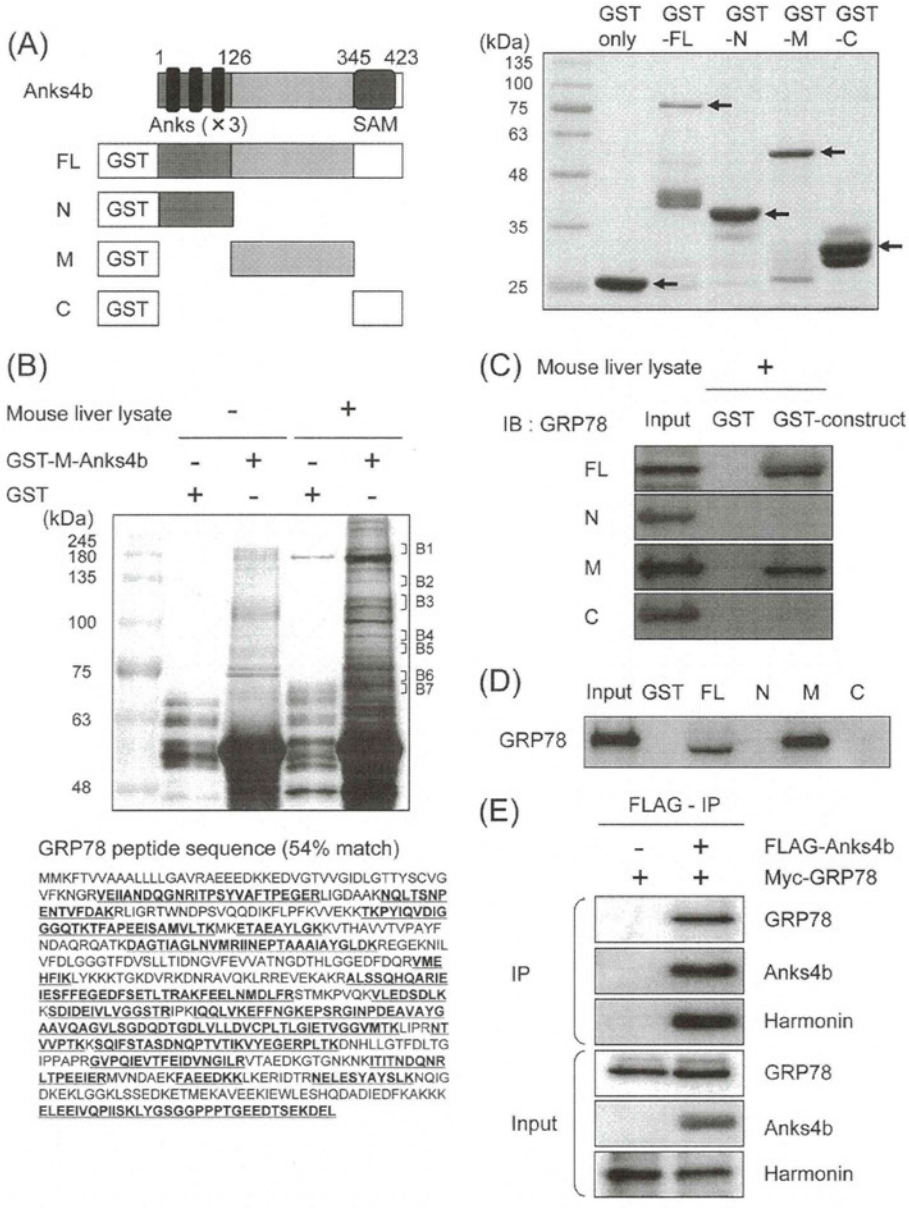

FIGURE 4. **Interaction of Anks4b and GRP78 *in vitro* and *in vivo*.** *A*, schematic representation of full-length Anks4b (*FL*) and deletion mutants of Anks4b (N-Anks4b (*N*), M-Anks4b (*M*), and C-Anks4b (*C*)) and expression of GST-Anks4b fusion proteins (Coomassie Brilliant Blue staining). *SAM*, sterile α motif. *B*, purification of proteins interacting with Anks4b. The GST pulldown assay using M-Anks4b was performed with mouse liver lysates. Eluted proteins were resolved by SDS-PAGE and then silver-stained. Seven regions (*B1–B7*) were excised for mass spectrometry. GRP78 residues were detected by mass spectrometry (*bold* and *underlined letters*). *C* and *D*, interaction of Anks4b and GRP78 *in vitro*. After the pulldown assay using mouse liver lysates (*C*) or MIN6 lysates (*D*), binding of GRP78 with FL- and M-Anks4b was detected by Western blotting (*IB*). *E*, interaction of Anks4b and GRP78 *in vivo*. COS-7 cells were transfected with the pCMV-Bip/GRP78-Myc-KDEL-wt or pCMV-Bip/GRP78-Myc-KDEL-wt and pcDNA3-FLAG-Anks4b expression vectors. Immunoprecipitation (*IP*) was performed with FLAG resin and 700 μg of COS-7 cell lysate.

unknown. To elucidate the role of Anks4b in β-cells, we searched for molecules that interacted with full-length Anks4b (FL) and with its deletion mutants (N-, M-, and C-Anks4b) (Fig. 4*A*) by performing a GST pulldown assay of mouse liver lysates (Fig. 4*B* and supplemental Fig. 4). We found a protein of ~75 kDa that specifically precipitated with GST-M-Anks4b (B6), and it was identified as GRP78/binding immunoglobulin protein (BiP) by mass spectrometry (Fig. 4*B*). GRP78 is an ER-localized chaperone protein that is induced by the unfolded protein response in response to ER stress (26, 27). Binding of GRP78 to GST-FL-Anks4b and GST-M-Anks4b, but not to GST, GST-N-Anks4b, or C-Anks4b, was confirmed by Western blotting using a specific antibody for GRP78 (Fig. 4*C*), suggesting that GRP78 bound to the middle region of Anks4b. GST pulldown experiments using MIN6 cell lysates also demonstrated binding of GRP78 to Anks4b (Fig. 4*D*).

Subsequently, we evaluated the interaction between Anks4b and GRP78 in cultured cells. COS-7 cells were transfected with the Myc-GRP78 expression plasmid alone or with Myc-GRP78 plus FLAG-tagged wild-type Anks4b expression plasmids, and

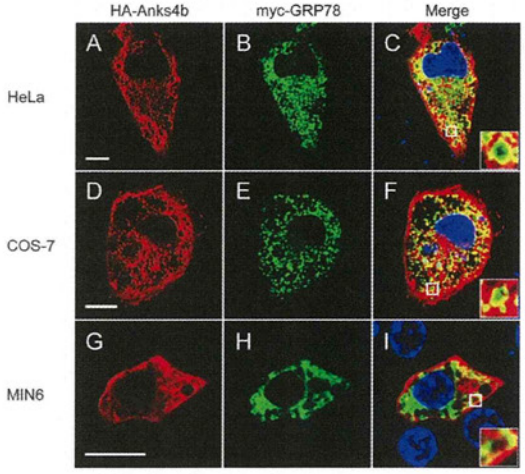

FIGURE 5. **Intracellular localization of Anks4b adjacent to the ER membrane.** *A–I*, HeLa (*A–C*), COS-7 (*D–F*), and MIN6 (*G–I*) cells were cotransfected with the pcDNA3-HA-Anks4b and pCMV-Bip/GRP78-Myc-KDEL-wt expression vectors. Cells were double-stained with anti-HA antibody (Alexa Fluor 563, *red*) and anti-Myc antibody (Alexa Fluor 488, *green*). DAPI (*blue*) was used for nuclear staining. *Insets* represent higher magnifications of the *boxed regions* in *C* (×18), *F* (×13), and *I* (×8). *Scale bar* = 10 μm.

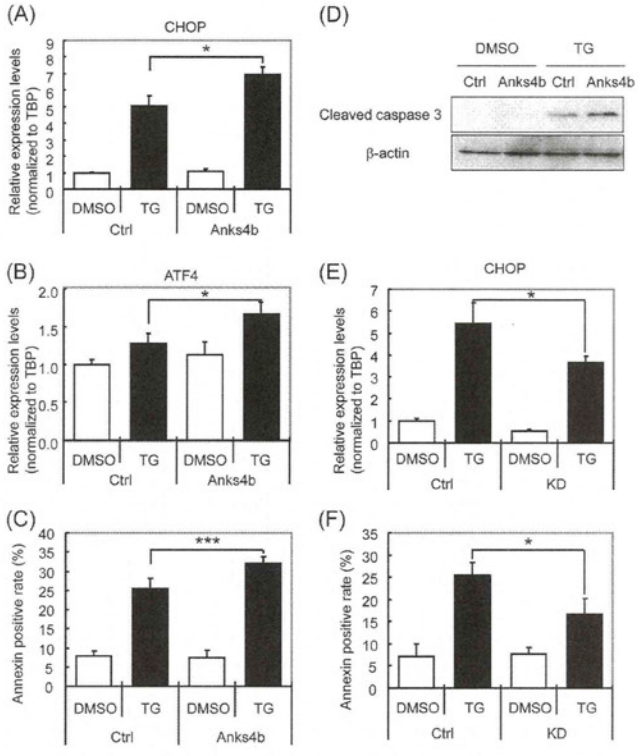

FIGURE 6. **Regulation of ER stress-mediated apoptosis by Anks4b.** *A* and *B*, MIN6 cells overexpressing Anks4b were cultured in the absence or presence of 1 μM thapsigargin for 20 h, and then quantitative RT-PCR was performed. *TBP*, TATA-binding protein. *DMSO*, dimethyl sulfoxide; *Ctrl*, control. *C*, MIN6 cells overexpressing Anks4b were cultured in the absence or presence of 1 μM thapsigargin for 30 h, and the percentage of annexin V-positive cells was analyzed by flow cytometry. *D*, Western blotting of cleaved caspase-3 after treatment with 1 μM thapsigargin for 20 h. *E*, Anks4b knockdown MIN6 cells were cultured for 20 h with 1 μM thapsigargin, and then quantitative RT-PCR was performed. *F*, annexin V-positive cells were analyzed after treatment of Anks4b knockdown MIN6 cells with 1 μM thapsigargin for 30 h. The mean ± S.D. for each group ($n = 4$) is shown (*, $p < 0.05$, **, $p < 0.01$, ***, $p < 0.001$).

cell lysates were immunoprecipitated with FLAG resin. As shown in Fig. 4*E*, FLAG-Anks4b was able to coimmunoprecipitate GRP78 as well as harmonin, a protein that was previously found to interact with Anks4b (25). These results indicated that Anks4b binds to GRP78 in cells.

Anks4b Colocalizes with GRP78 in the Endoplasmic Reticulum—We next investigated the intracellular localization of Anks4b. HA-tagged Anks4b and Myc-tagged GRP78 constructs were cotransfected into HeLa cells, and an immunofluorescence study was performed. HA staining (Anks4b, *red*) revealed a reticular pattern in the cytoplasm, but no signals were detected in the nucleus (Fig. 5*A*). Double staining for Anks4b and GRP78 (Myc, *green*) as a marker for the ER revealed that both signals were frequently colocalized (Fig. 5, *B* and *C*). In contrast, Anks4b staining did not overlap with MitoTracker, a specific marker for the mitochondria (supplemental Fig. 5). A similar staining pattern was also detected in COS-7 cells and MIN6 cells (Fig. 5, *D–I*). These findings were further evidence that Anks4b interacts with GRP78. Notably, Anks4b staining was detected at the periphery of the ER lumen (Fig. 5, *C*, *F*, and *I*, *inset*), suggesting that it was localized adjacent to the ER membrane.

Anks4b Regulates Apoptosis in Response to ER Stress—GRP78 is a major chaperone protein that protects cells from ER stress, and overexpression of GRP78 reduces ER stress-mediated apoptosis by attenuating the expression of C/EBP homologous protein (CHOP) (28, 29). Accordingly, detection of an interaction between Anks4b and GRP78 prompted us to investigate the role of Anks4b in both ER stress and apoptosis. TG causes ER stress by preventing calcium uptake from the cytoplasm into the ER (30), and treatment of MIN6 cells with 1 μM TG for 20 h increased the expression of the ER stress-related genes (ATF4, spliced XBP1, and CHOP) (data not shown). First, we examined the effect of Anks4b overexpression on MIN6 cells (supplemental Fig. 6). Anks4b overexpression did not affect CHOP gene expression in the absence of TG, but TG-induced CHOP expression was significantly increased (1.4-fold, $p < 0.05$) (Fig. 6*A*). TG-induced ATF4 expression was also significantly augmented in Anks4b-overexpressing MIN6 cells (1.3-fold, $p < 0.05$) (Fig. 6*B*). Furthermore, the number of annexin V-positive apoptotic cells was increased by overexpression of Anks4b (1.3-fold, $p < 0.001$) (Fig. 6*C*). Augmentation of apoptosis was also observed in MIN6 cells overexpressing HNF4α7 (supplemental Fig. 7). Activation of caspase-3 mediates the induction of apoptosis downstream of CHOP (31), and activated (cleaved) caspase-3 protein expression was increased when Anks4b-overexpessing MIN6 cells were treated with TG (Fig. 6*D*).

Next, we examined the effect of knockdown of Anks4b in MIN6 cells (supplemental Fig. 8). Suppression of endogenous Anks4b mRNA by shRNA in MIN6 (reduced to 40.5% of the control level) did not affect CHOP gene expression in the absence of TG, but TG-induced CHOP expression was significantly reduced by 32.1% ($p < 0.05$) (Fig. 6*E*). In addition, flow cytometric analysis using annexin V revealed that TG-induced apoptosis was also decreased by suppression of Anks4b (Fig. 6*F*). Collectively, these findings indicate that Anks4b promotes the induction of ER stress and apoptosis by TG in MIN6 cells.

DISCUSSION

HNF4α plays an important role in pancreatic β-cells, and mutation of this gene causes MODY1 (6). However, there has been little information available about the target genes of HNF4α in β-cells. We and others have previously reported that most of the genes involved in glucose metabolism, including *Slc2a2*, *Gck*, *Kcnj11*, *Abcc8*, and *Ins*, are not differentially expressed in βHNF4α KO islets (7, 8, 19). The present large scale expression profiling analysis also demonstrated that expression of genes known to be involved in insulin secretion was largely unchanged in HNF4α deficient islets. Like HNF4α, mutation of the HNF1α gene also causes a form of MODY (MODY3), which is characterized by β-cell dysfunction (21). Expression of many genes involved in insulin secretion, including *Slc2a2*, *Pklr*, and *Tmem27*, is decreased in HNF1α KO islets (22, 32, 33). Thus, the gene expression pattern of HNF4α KO islets differs markedly from that of HNF1α KO islets.

In the present study, we found that Anks4b gene expression was markedly reduced in both βHNF4α KO islets and HNF4α KD-MIN6 cells. Reporter gene assays and ChIP analysis demonstrated that HNF4α bound to a conserved HNF4 binding motif and activated transcription, thus indicating that Anks4b is a direct target of HNF4α in β-cells. In addition to the pancreatic islets, Anks4b is also expressed in the liver, kidney, small intestine, and colon (25). This distribution of expression is very similar to that of HNF4α, suggesting that HNF4α plays a role in Anks4b gene transcription in these tissues. Furthermore, we found that Anks4b gene expression was also regulated by HNF1α. Cotransfection of HNF4α and HNF1α dramatically stimulated promoter activity when compared with the sum of the effects of each transcription factor acting separately (Fig. 3*D*). Recently, Boj *et al.* (34) reported that HNF4α and HNF1α regulate common target genes through interdependent regulatory mechanisms. Although the mechanism of the functional interaction between HNF4α and HNF1α is still unclear, our results indicate that Anks4b gene expression is another example of such interdependent regulation.

Anks4b was originally identified as harmonin (the gene responsible for Usher deafness syndrome type 1C)-interacting protein, but its function is unknown. In this study, we showed that Anks4b binds to GRP78, a major ER chaperone protein. We also found that Anks4b knockdown significantly inhibited TG-induced CHOP expression and apoptosis in MIN6 cells, whereas Anks4b overexpression enhanced TG-induced CHOP expression and apoptosis, strongly suggesting a direct role of Anks4b in increasing the susceptibility of β-cells to ER stress and apoptosis. Investigation of Anks4b knock-out mice will improve our understanding of the role of this molecule in ER stress. Anks4b does not possess the canonical ER localization signal (35), so the molecular mechanism by which Anks4b binds to GRP78 and regulates ER stress warrants further investigation.

HNF4α plays an important role in a number of metabolic pathways, including those for gluconeogenesis, ureagenesis, fatty acid metabolism, and drug metabolism (36–38). Our finding that Anks4b is a target of HNF4α uncovers a new role for this transcription factor in regulating β-cell susceptibility to ER stress. ER stress is associated with β-cell apoptosis in common type 2 diabetes (39). Because reduced expression of Anks4b was associated with a decrease, rather than an increase, of ER stress and apoptosis, the significance of Anks4b in relation to the occurrence of MODY is unclear. However, recent genetic studies have shown that HNF4α has dual opposing roles in the β-cell during different periods of life. Although HNF4α deficiency results in diabetes in young adults (6), the same genetic defect occasionally causes hyperinsulinemic hypoglycemia at birth (40, 41). Further studies will need to address whether reduced Anks4b expression is responsible for the hypersecretion of β-cells early in life.

In conclusion, we identified Anks4b as a novel molecule that controls the susceptibility to ER stress-induced apoptosis. The ER is critical for the normal functioning of pancreatic β-cells, and ER stress-associated apoptosis is often a contributory factor to β-cell death in type 2 diabetes (39). Therefore, Anks4b may be a potential target for the treatment of diabetes associated with ER stress.

Acknowledgments—We thank Prof. J. Miyazaki (Osaka University) for the gift of MIN6 cells, Prof. T. Kitamura (Tokyo University) for providing the Plat-E cells and pMXs vector, and Dr. T. Tanaka (Tokyo University) for providing pcDNA3-HNF4α7 plasmid.

REFERENCES

1. Sladek, F. M., Zhong, W. M., Lai, E., and Darnell, J. E. (1990) Liver-enriched transcription factor HNF-4 is a novel member of the steroid hormone receptor superfamily. *Genes Dev.* **4,** 2353–2365
2. Nammo, T., Yamagata, K., Tanaka, T., Kodama, T., Sladek, F. M., Fukui, K., Katsube, F., Sato, Y., Miyagawa, J., and Shimomura, I. (2008) Expression of HNF-4α (MODY1), HNF-1β (MODY5), and HNF-1α (MODY3) proteins in the developing mouse pancreas. *Gene Expr. Patterns* **8,** 96–106
3. Hadzopoulou-Cladaras, M., Kistanova, E., Evagelopoulou, C., Zeng, S., Cladaras, C., and Ladias, J. A (1997) Functional domains of the nuclear receptor hepatocyte nuclear factor 4. *J. Biol. Chem.* **272,** 539–550
4. Ihara, A., Yamagata, K., Nammo, T., Miura, A., Yuan, M., Tanaka, T., Sladek, F. M., Matsuzawa, Y., Miyagawa, J., and Shimomura, I. (2005) Functional characterization of the HNF4α isoform (HNF4α8) expressed in pancreatic β-cells. *Biochem. Biophys. Res. Commun.* **329,** 984–990
5. Bell, G. I., and Polonsky, K. S. (2001) Diabetes mellitus and genetically programmed defects in β-cell function. *Nature* **414,** 788–791
6. Yamagata, K., Furuta, H., Oda, N., Kaisaki, P. J., Menzel, S., Cox, N. J., Fajans, S. S., Signorini, S., Stoffel, M., and Bell, G. I. (1996) Mutations in the hepatocyte nuclear factor-4α gene in maturity-onset diabetes of the young (MODY1) *Nature* **384,** 458–460
7. Miura, A., Yamagata, K., Kakei, M., Hatakeyama, H., Takahashi, N., Fukui, K., Nammo, T., Yoneda, K., Inoue, Y., Sladek, F. M., Magnuson, M. A., Kasai, H., Miyagawa, J., Gonzalez, F. J., and Shimomura, I. (2006) Hepatocyte nuclear factor-4α is essential for glucose-stimulated insulin secretion by pancreatic β-cells. *J. Biol. Chem.* **281,** 5246–5257
8. Gupta, R. K., Vatamaniuk, M. Z., Lee, C. S., Flaschen, R. C., Fulmer, J. T., Matschinsky, F. M., Duncan, S. A., and Kaestner, K. H. (2005) The MODY1 gene HNF-4α regulates selected genes involved in insulin secretion. *J. Clin. Invest.* **115,** 1006–1015
9. Hayhurst, G. P., Lee, Y. H., Lambert, G., Ward, J. M., and Gonzalez, F. J. (2001) Hepatocyte nuclear factor 4α (nuclear receptor 2A1) is essential for maintenance of hepatic gene expression and lipid homeostasis. *Mol. Cell Biol.* **21,** 1393–1403
10. Rhee, J., Inoue, Y., Yoon, J. C., Puigserver, P., Fan, M., Gonzalez, F. J., and Spiegelman, B. M. (2003) Regulation of hepatic fasting response by PPARγ coactivator-1α (PGC-1): requirement for hepatocyte nuclear factor 4α in gluconeogenesis. *Proc. Natl. Acad. Sci. U.S.A.* **100,** 4012–4017

11. Wang, H., Maechler, P., Antinozzi, P. A., Hagenfeldt, K. A., and Wollheim, C. B. (2000) Hepatocyte nuclear factor 4α regulates the expression of pancreatic β-cell genes implicated in glucose metabolism and nutrient-induced insulin secretion. *J. Biol. Chem.* **275,** 35953–35959
12. Sato, Y., Endo, H., Okuyama, H., Takeda, T., Iwahashi, H., Imagawa, A., Yamagata, K., Shimomura, I., and Inoue, M. (2011) Cellular hypoxia of pancreatic β-cells due to high levels of oxygen consumption for insulin secretion in vitro. *J. Biol. Chem.* **286,** 12524–12532
13. Miyazaki, J., Araki, K., Yamato, E., Ikegami, H., Asano, T., Shibasaki, Y., Oka, Y., and Yamamura, K. (1990) Establishment of a pancreatic β-cell line that retains glucose-inducible insulin secretion: special reference to expression of glucose transporter isoforms. *Endocrinology* **127,** 126–132
14. Yang, Q., Yamagata, K., Yamamoto, K., Cao, Y., Miyagawa, J., Fukamizu, A., Hanafusa, T., and Matsuzawa, Y. (2000) R127W-HNF-4α is a loss-of-function mutation but not a rare polymorphism and causes type II diabetes in a Japanese family with MODY1. *Diabetologia* **43,** 520–524
15. Yamagata, K., Yang, Q., Yamamoto, K., Iwahashi, H., Miyagawa, J., Okita, K., Yoshiuchi, I., Miyazaki, J., Noguchi, T., Nakajima, H., Namba, M., Hanafusa, T., and Matsuzawa, Y. (1998) Mutation P291fsinsC in the transcription factor hepatocyte nuclear factor-1α is dominant negative. *Diabetes* **47,** 1231–1235
16. Dignam, J. D., Lebovitz, R. M., and Roeder, R. G. (1983) Accurate transcription initiation by RNA polymerase II in a soluble extract from isolated mammalian nuclei. *Nucleic Acids Res.* **11,** 1475–1489
17. Shevchenko, A., Wilm, M., Vorm, O., and Mann, M. (1996) Mass spectrometric sequencing of proteins silver-stained polyacrylamide gels. *Anal. Chem.* **68,** 850–858
18. Kitamura, T., Koshino, Y., Shibata, F., Oki, T., Nakajima, H., Nosaka, T., and Kumagai, H. (2003) Retrovirus-mediated gene transfer and expression cloning: powerful tools in functional genomics. *Exp. Hematol.* **31,** 1007–1014
19. Gupta, R. K., Gao, N., Gorski, R. K., White, P., Hardy, O. T., Rafiq, K., Brestelli, J. E., Chen, G., Stoeckert, C. J., Jr., and Kaestner, K. H. (2007) Expansion of adult β-cell mass in response to increased metabolic demand is dependent on HNF-4α. *Genes Dev.* **21,** 756–769
20. Pontoglio, M., Barra, J., Hadchouel, M., Doyen, A., Kress, C., Bach, J. P., Babinet, C., and Yaniv, M. (1996) Hepatocyte nuclear factor 1 inactivation results in hepatic dysfunction, phenylketonuria, and renal Fanconi syndrome. *Cell* **84,** 575–585
21. Yamagata, K., Oda, N., Kaisaki, P. J., Menzel, S., Furuta, H., Vaxillaire, M., Southam, L., Cox, R. D., Lathrop, G. M., Boriraj, V. V., Chen, X., Cox, N. J., Oda, Y., Yano, H., Le Beau, M. M., Yamada, S., Nishigori, H., Takeda, J., Fajans, S. S., Hattersley, A. T., Iwasaki, N., Hansen, T., Pedersen, O., Polonsky, K. S., and Bell, G. I. (1996) Mutations in the hepatocyte nuclear factor-1α gene in maturity-onset diabetes of the young (MODY3) *Nature* **384,** 455–458
22. Servitja, J. M., Pignatelli, M., Maestro, M. A., Cardalda, C., Boj, S. F., Lozano, J., Blanco, E., Lafuente, A., McCarthy, M. I., Sumoy, L., Guigó, R., and Ferrer, J. (2009) Hnf1α (MODY3) controls tissue-specific transcriptional programs and exerts opposed effects on cell growth in pancreatic islets and liver. *Mol. Cell Biol.* **29,** 2945–2959
23. Ozeki, T., Takahashi, Y., Kume, T., Nakayama, K., Yokoi, T., Nunoya, K., Hara, A., and Kamataki, T. (2001) Cooperative regulation of the transcription of human dihydrodiol dehydrogenase (*DD*)*4*/aldo-keto reductase (*AKR*)*1C4* gene by hepatocyte nuclear factor (HNF)-4α/γ and HNF-1α. *Biochem. J.* **355,** 537–544
24. Eeckhoute, J., Formstecher, P., and Laine, B. (2004) Hepatocyte nuclear factor 4α enhances the hepatocyte nuclear factor 1α-mediated activation of transcription. *Nucleic Acids Res.* **32,** 2586–2593
25. Johnston, A. M., Naselli, G., Niwa, H., Brodnicki, T., Harrison, L. C., and Góñez, L. J. (2004) Harp (harmonin-interacting, ankyrin repeat-containing protein), a novel protein that interacts with harmonin in epithelial tissues. *Genes Cells* **9,** 967–982
26. Zhang, L. H., and Zhang, X. (2010) Roles of GRP78 in physiology and cancer. *Journal of cellular biochemistry* **110,** 1299–1305
27. Wang, M., Wey, S., Zhang, Y., Ye, R., and Lee, A. S. (2009) Role of the unfolded protein response regulator GRP78/BiP in development, cancer, and neurological disorders. *Antioxid. Redox Signal.* **11,** 2307–2316
28. Morris, J. A., Dorner, A. J., Edwards, C. A., Hendershot, L. M., and Kaufman, R. J. (1997) Immunoglobulin-binding protein (BiP) function is required to protect cells from endoplasmic reticulum stress but is not required for the secretion of selective proteins. *J. Biol. Chem.* **272,** 4327–4334
29. Wang, X. Z., Lawson, B., Brewer, J. W., Zinszner, H., Sanjay, A., Mi, L. J., Boorstein, R., Kreibich, G., Hendershot, L. M., and Ron, D. (1996) Signals from the stressed endoplasmic reticulum induce C/EBP-homologous protein (CHOP/GADD153). *Mol. Cell Biol.* **16,** 4273–4280
30. Treiman, M., Caspersen, C., and Christensen, S. B. (1998) A tool coming of age: thapsigargin as an inhibitor of sarco-endoplasmic reticulum Ca^{2+}-ATPases. *Trends Pharmacol. Sci.* **19,** 131–135
31. Lai, E., Teodoro, T., and Volchuk, A. (2007) Endoplasmic reticulum stress: signaling the unfolded protein response. *Physiology* **22,** 193–201
32. Fukui, K., Yang, Q., Cao, Y., Takahashi, N., Hatakeyama, H., Wang, H., Wada, J., Zhang, Y., Marselli, L., Nammo, T., Yoneda, K., Onishi, M., Higashiyama, S., Matsuzawa, Y., Gonzalez, F. J., Weir, G. C., Kasai, H., Shimomura, I., Miyagawa, J., Wollheim, C. B., and Yamagata, K. (2005) The HNF-1 target collectrin controls insulin exocytosis by SNARE complex formation. *Cell Metab.* **2,** 373–384
33. Akpinar, P., Kuwajima, S., Krützfeldt, J., and Stoffel, M. (2005) Tmem27: a cleaved and shed plasma membrane protein that stimulates pancreatic β-cell proliferation. *Cell Metab.* **2,** 385–397
34. Boj, S. F., Petrov, D., and Ferrer, J. (2010) Epistasis of transcriptomes reveals synergism between transcriptional activators Hnf1α and Hnf4α. *PLoS genet.* **6,** e1000970
35. Pagny, S., Lerouge, P., Faye, L., and Gomord, V. (1999) Signals and mechanisms for protein retention in the endoplasmic reticulum. *J. Exp. Bot.* **50,** 157–164
36. Sladek, F. M., and Seidel, S. D. (2001) in *Nuclear Receptors and Genetic Diseases* (Burris, T. P., and McCabe, E., eds) pp. 309–361, Academic Press, London, UK
37. Gonzalez, F. J. (2008) Regulation of hepatocyte nuclear factor 4α-mediated transcription. *Drug Metab. Pharmacokinet.* **23,** 2–7
38. Bolotin, E., Liao, H., Ta, T. C., Yang, C., Hwang-Verslues, W., Evans, J. R., Jiang, T., and Sladek, F. M. (2010) Integrated approach for the identification of human hepatocyte nuclear factor 4α target genes using protein binding microarrays. *Hepatology* **51,** 642–653
39. Marchetti, P., Bugliani, M., Lupi, R., Marselli, L., Masini, M., Boggi, U., Filipponi, F., Weir, G. C., Eizirik, D. L., and Cnop, M. (2007) The endoplasmic reticulum in pancreatic β-cells of type 2 diabetes patients. *Diabetologia* **50,** 2486–2494
40. Pearson, E. R., Boj, S. F., Steele, A. M., Barrett, T., Stals, K., Shield, J. P., Ellard, S., Ferrer, J., and Hattersley, A. T. (2007) Macrosomia and hyperinsulinemic hypoglycemia in patients with heterozygous mutations in the HNF4A gene. *PLoS Med.* **4,** e118
41. Kapoor, R. R., Locke, J., Colclough, K., Wales, J., Conn, J. J., Hattersley, A. T., Ellard, S., and Hussain, K. (2008) Persistent hyperinsulinemic hypoglycemia and maturity-onset diabetes of the young due to heterozygous HNF4A mutations. *Diabetes* **57,** 1659–1663

BRAIN RESEARCH 1453 (2012) 26–33

Available online at www.sciencedirect.com

SciVerse ScienceDirect

www.elsevier.com/locate/brainres

BRAIN RESEARCH

Research Report

RGS2 mediates the anxiolytic effect of oxytocin

Naoki Okimoto[a,b], Oliver J. Bosch[c], David A. Slattery[c], Konstanze Pflaum[c], Hiroaki Matsushita[a], Fan-Yan Wei[d], Masayasu Ohmori[a], Tei-ichi Nishiki[a], Iori Ohmori[a], Yuji Hiramatsu[b], Hideki Matsui[a], Inga D. Neumann[c], Kazuhito Tomizawa[d,*]

[a]Department of Physiology, Okayama University Graduate School of Medicine, Dentistry and Pharmaceutical Sciences, Okayama 700–8558, Japan
[b]Department of Obstetrics & Gynecology, Okayama University Graduate School of Medicine, Dentistry and Pharmaceutical Sciences, Okayama 700–8558, Japan
[c]Department of Neurobiology and Animal Physiology, University of Regensburg, Regensburg 93040, Germany
[d]Department of Molecular Physiology, Faculty of Life Sciences, Kumamoto University, Kumamoto 860–8556, Japan

ARTICLE INFO

Article history:
Accepted 4 March 2012
Available online 13 March 2012

Keywords:
Anxiety
Stress
Amygdala
Female
Mouse

ABSTRACT

The neuropeptide oxytocin (OT) has been shown to exert multiple functions in both males and females, and to play a key role in the regulation of emotionality in the central nervous system (CNS). OT has an anxiolytic effect in the CNS of rodents and humans. However, the molecular mechanisms of this effect are unclear. Here we show that OT induced the expression of regulator of G-protein signaling 2 (RGS2), a regulatory factor for anxiety, in the central amygdala (CeA) of female mice. Bath application of OT increased RGS2 levels in slices of the amygdala of virgin mice. RGS2 levels in the CeA were higher in lactating mice than in virgin mice. In contrast, RGS2 levels in mice that had given birth did not increase when the pups were removed. Acute restraint stress for 4 h induced RGS2 expression within the CeA, and local administration of an OT receptor antagonist inhibited this expression. Behavioral experiments revealed that transient restraint stress had an anxiolytic effect in wild-type females, and RGS2 levels in the CeA correlated with the anxiolytic behavior. By contrast, in the OT receptor-deficient mice, restraint stress neither increased RGS2 levels in the CeA nor had an anxiolytic effect. These results suggest that OT displays an anxiolytic effect through the induction of RGS2 expression in the CNS.

1. Introduction

OT is the classical reproductive hormone in female mammals, promoting uterine contractions during labor and milk ejection during lactation (Gainer and Wray, 1994; Neumann, 2001). OT also acts as a neurotransmitter/neuromodulator to regulate a range of central nervous system functions in both males and females, including emotional (Neumann, 2008), parental (Numan and Insel, 2003), affiliative (Insel and Shapiro, 1992), and sexual (Argiolas and Gessa, 1991) behaviors, as well as spatial and social cognition (Bielsky and Young, 2004; Tomizawa et al., 2003). Moreover, OT is an important regulator of anxiety (Bale et al., 2001; Blume et al., 2008; Neumann et al., 2000a) and of stress-coping circuitries (Ebner et al., 2005; Huber et al., 2005). For instance, OT released in the hypothalamus mediates mating-induced anxiolysis in rats (Waldherr and Neumann, 2007). Psycho-social or physical stressors like forced swimming and restraint stress evoke the release of OT in various areas

* *Corresponding author at:* Department of Molecular Physiology, Faculty of Life Sciences, Kumamoto University, 1-1-1 Honjyo, Kumamoto 860–8556, Japan. Fax: +81 96 373 5052.
E-mail address: tomikt@kumamoto-u.ac.jp (K. Tomizawa).

0006-8993/$ – see front matter © 2012 Elsevier B.V. All rights reserved.
doi:10.1016/j.brainres.2012.03.012

known to be involved in the modulation of stress mechanisms, including the amygdala and the hypothalamic supraoptic (SON) and paraventricular (PVN) nuclei (Ebner et al., 2000; Ebner et al., 2005; Wigger and Neumann, 2002). In humans, moreover, intranasal OT promotes trust, and reduces the level of anxiety, possibly at the level of the amygdala (Heinrichs et al., 2003; Kirsch et al., 2005; Kosfeld et al., 2005; Labuschagne et al., 2010; Slattery and Neumann, 2010).

The amygdala is a region of the brain particularly relevant to the processing of behavioral and neuroendocrinal stress responses (Gray, 1996), especially with respect to the oxytocinergic system (Bale et al, 2001; Neumann et al, 2000a). Within the amygdala, specifically in the medial and central (CeA) subnuclei, a substantial number of oxytocinergic fibers (Sofroniew, 1983) and OT receptors have been detected (Barberis and Tribollet, 1996; Gimpl and Fahrenholz, 2001), suggesting that locally released OT is a potential mediator of the complex stress response. Indeed, local blockade of OT receptors within the amygdala resulted not only in altered emotionality (Bale et al, 2001; Neumann, 2002) but also in a dis-inhibition of the hypothalamo-pituitary-adrenal (HPA) axis of rats (Neumann et al, 2000b).

There is no doubt that OT in its activated state is an endogenous neuromodulator with an anxiolytic effect in response to stress. However, the precise mechanism of OT receptor-mediated effects and the involvement of subsequent intracellular signaling cascades, for example in the anxiolytic effects of OT, are only beginning to be elucidated (Blume et al., 2008). There is an OT receptor, which is a G-protein-coupled receptor (GPCR) that couples to a complex intracellular signaling pathway (van den Burg and Neumann, 2011). The binding of OT with the receptor activates the MAP kinase cascade both *in vitro* (Tomizawa et al., 2003) and *in vivo* (Blume et al, 2008) and induces the phosphorylation of cAMP response element-binding protein (CREB), a transcription factor critical to neuronal development, synaptic plasticity and memory formation (Han et al., 2007; Lonze et al., 2002; Tomizawa et al., 2003). These results suggest the anxiolytic effect of OT to occur through the regulation of gene expression.

Regulator of G-protein signaling (RGS) proteins are key modulators of G protein-coupled receptor signaling by virtue of their ability to accelerate the intrinsic GTP hydrolysis activity of G subunits (Hollinger and Hepler, 2002; Hollinger and Hepler, 2004). RGS2 was one of the first mammalian RGS proteins to be identified, (Siderovski et al., 1996) and stimulates GTPase activity through interaction with Gqα *in vitro* (Heximer et al., 1997; Hollinger and Hepler, 2002). Previous studies have shown that RGS2 modulates anxiety in both mice and humans (Cui et al., 2008; Flint, 2003; Oliveira-dos-Santos et al., 2000; Smoller et al., 2008; Yalcin et al., 2004). For instance, the use of transgenic and knockout mice as well as quantitative trait locus (QTL) techniques in the laboratory has led to the identification of candidate genes related to fear- and anxiety-related behaviors (Norrholm and Ressler, 2009). In mice, a QTL on chromosome 1 is associated with anxiety-related phenotypes (Flint, 2003); the principal quantitative trait gene for this linkage signal has been identified as *RGS2* (Yalcin et al., 2004). In addition, *RGS2* gene polymorphisms have been associated with panic disorder (Leygraf et al., 2006) and completed suicides (Cui et al., 2008).

The aim of the present study was to clarify the molecular mechanism behind the local anxiolytic effect of OT in the amygdala. We first identified RGS2 as a gene whose expression is up-regulated by OT and investigated whether RGS2 expression was increased in OT-applied amygdala slices and lactating mice. Moreover, we examined whether acute restraint stress induced OT secretion and RGS2 expression in CeA of female mice, resulting in an anxiolytic effect. Finally, a deficiency and blockade of the OT receptor was found to abrogate these effects of acute restraint stress.

2. Results

2.1. *Up-regulated genes in primary cultured neurons treated with oxytocin*

We first examined up-regulated genes in primary cultured neurons treated with OT by a microarray analysis. Five genes were up-regulated more than two-fold compared with control neurons (Table 1). The greatest increase was shown by the RGS2 gene (Table 1). Moreover, we examined up-regulated genes in the central amygdala (CeA) of lactating mice at postpartum 7 days by a microarray analysis. Only RGS2 was up-regulated more than two-fold among the five genes in the CeA of lactating mice compared with virgin mice (data not shown).

2.2. *Induction of RGS2 expression in the CeA by OT and during motherhood*

To investigate whether OT induced RGS2 expression in the CeA, amygdala slices were incubated with OT or PBS, and the RGS2 level in the CeA was examined by Western blotting. OT induced RGS2 expression in the CeA of virgin mice 60 and 120 min after the addition of OT (Fig. 1A). It was next examined whether the RGS2 level increased in the CeA during motherhood. The RGS2 level at 1 day postpartum was the same as that in virgin mice (Fig. 1B). However, the protein level was significantly increased at 3, 7 and 10 days postpartum (Fig. 1B). Interestingly, RGS2 levels were not increased in females when the pups were removed after labor (Fig. 1B). These results suggest that OT or other suckling- or birth-related factors such as prolactin may induce RGS2 expression in the CeA of female mice. Therefore, we next examined

Table 1 – Up-regulated genes in primary cultured neurons treated with oxytocin. Relative gene expression in OT-treated neurons compared with control neurons.

Gene Name	Fold change
Mus musculus regulator of G-protein signaling 2 (Rgs2), mRNA	4.70
PROTOCADHERIN PRECURSOR PCDH	3.28
Mus musculus brain derived neurotrophic factor (Bdnf), mRNA	3.02
Mus musculus host cell factor C1 (Hcfc1), mRNA	2.45
Mus musculus protein kinase C, epsilon (Prkce), mRNA	2.36

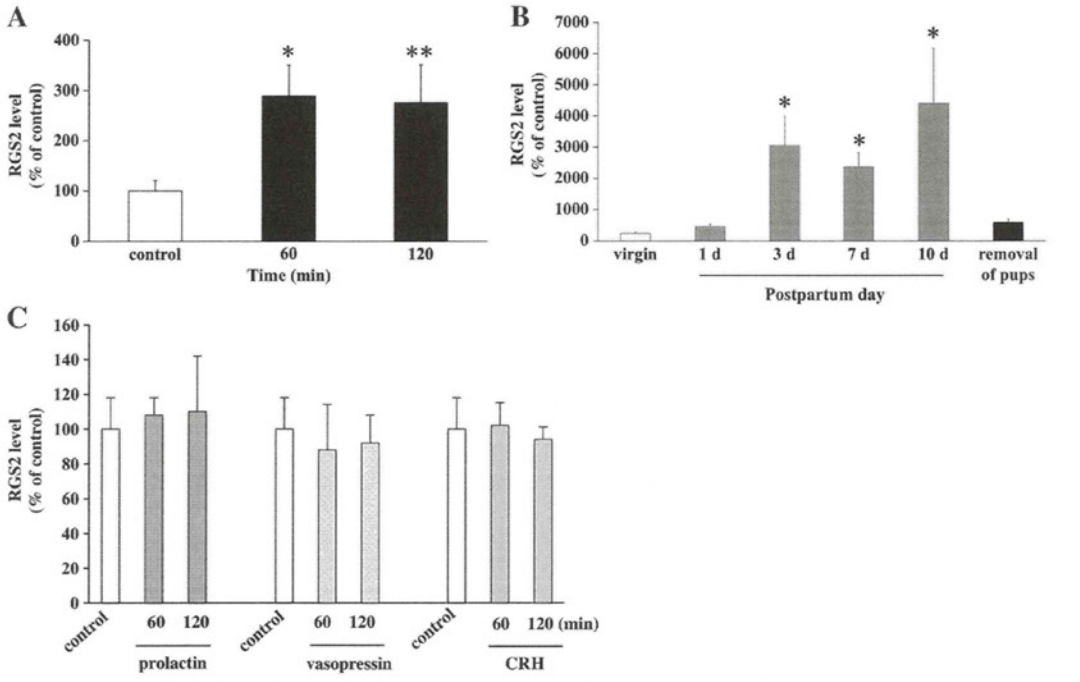

Fig. 1 – Induction of RGS2 expression in the CeA by OT treatment (A) and during motherhood (B) but not by prolactin, vasopressin or CRH (C). (A) Amygdala slices of female mice were incubated with OT for 60 and 120 min. As a control, the slices were incubated with ACSF. The RGS2 level in the CeA was examined by Western blotting. n=4–5 each. * $P<0.01$, ** $P<0.05$ *v.s.* control. (B) The CeA of lactating mice or of lactating mice whose pups were removed immediately after birth was taken out on the days indicated after birth, and RGS2 levels were compared with those in age-matched virgin mice (virgin). n=4–5 each. * $P<0.001$ *v.s.* age-matched virgin mice (virgin). (C) Amygdala slices of female mice were incubated with prolactin, vasopressin and CRH for 60 and 120 min. As a control, the slices were incubated with ACSF. The RGS2 level in the CeA was examined by Western blotting. n=5 each.

whether prolactin, vasopressin and corticotropin-releasing hormone (CRH) induced RGS2 expression in CeA slices. Incubation with the hormones had no effect on RGS2 levels (Fig. 1C).

2.3. *Induction of RGS2 level by restraint stress*

Stress exposure such as a 10-min forced swimming session causes a significant increase in OT release in the amygdala (Ebner et al., 2005). We next examined the effect of restraint stress on the RGS2 protein level in the CeA of female mice. The mice were restricted for 4 h per day. Restraint stress for 3 and 7 days significantly induced production of the protein (Fig. 2A) and the expression of the mRNAs (Fig. 2B) in the CeA.

To investigate whether OT mediated the restraint stress-induced RGS2 expression in the CeA, the effect of the OTR antagonist on the protein and mRNA levels was examined. The antagonist had no effect on normal RGS2 levels in the CeA (Fig. 2C), but inhibited the restraint stress-induced RGS2 expression (Fig. 2C). As a result, the protein level was decreased to that in control mice.

2.4. *Anxiolytic effect of short-term restraint stress*

It was next examined whether the repeated restraint stress protocol, shown to trigger RGS2 expression in the CeA, alters anxiety-related behavior in female mice. Females were subjected to restraint stress (4 h/day) for 2 days and anxiety-related behavior was tested in the elevated plus-maze 24 h later. Anxiolytic behavior was evaluated based on the time spent in the open arms. Mice exposed twice to restraint stress spent significantly more time in the open arms (control, 22.5±2.7%; Stress (+), 29.4±3.6%) (Fig. 3A), suggesting that stress exposure reduced anxiety in female mice. In mice exposed to restraint stress, the number of entries in the closed arms was the same as that of control mice (control, 12.5±2.3; Stress (+), 13.3±3.9%, $P>0.05$), suggesting the locomotor activity of the mice exposed to restraint stress to be the same as that of control mice.

We next examined whether the RGS2 level in the CeA was correlated with anxiety-related behavior (i.e. % time spent in the open arms). Females subjected to restraint stress for 2 days were tested in an elevated plus-maze and the RGS2 level in the CeA was examined. The RGS2 level correlated with anxiolytic behavior (Pearson's rank correlation, R squared=0.0537, 0.39, $P=0.0067$). (Fig. 3B).

2.5. *No anxiolytic effect of restrain stress in OTR KO mice*

To investigate whether OT mediates the anxiolytic effect of restraint stress, OTR KO mice were twice subjected to restraint stress (4 h/day) for 2 consecutive days. On day 3, 24 h after the

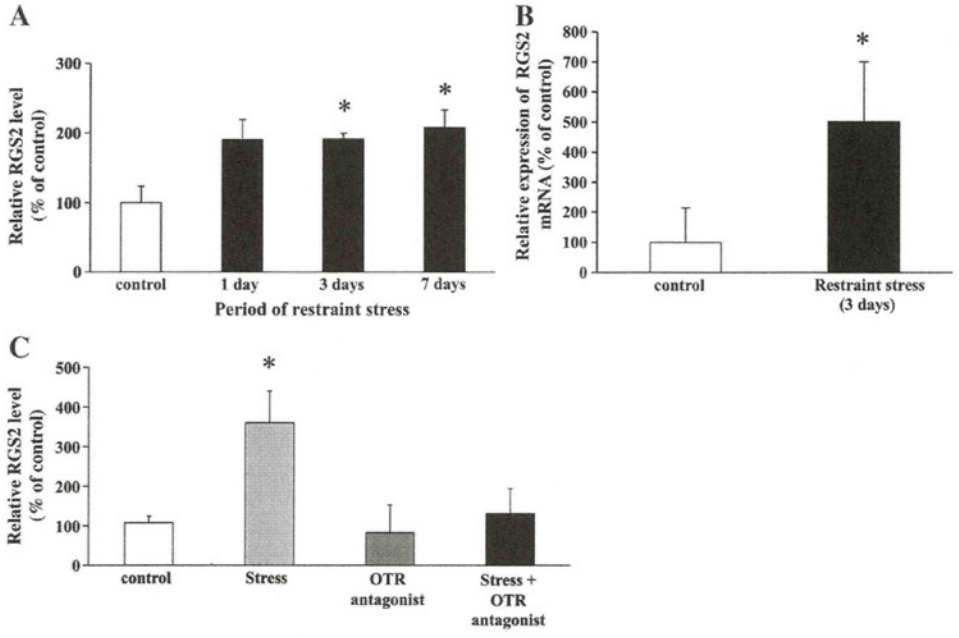

Fig. 2 – Effect of restraint stress on RGS2 protein and mRNA levels in the CeA of female mice. (A) Female mice were subjected to restraint stress (4 h per day) for the indicated period. The amygdala was removed 24 h after the last restrain stress. n = 6–7 each. (B) Effect of restraint stress on the expression of RGS2 mRNA. The mice were subjected to restraint stress (4 h per day) for 3 days (3 d). The amygdala was removed 24 h after the last stress. n = 8 each. (C) Effect of an OTR antagonist on the restraint stress-induced RGS2 expression. The antagonist (5 ng) was injected into the bilateral amygdala every 24 h for 5 days. Mice were subjected to restraint stress (4 h/day) 24 h after the first injection of the antagonist for 4 successive days. Twenty-four hours after the last restraint stress, the bilateral amygdalas were removed. As controls, mice were injected with vehicle (PBS). n = 7–10 each. * $P < 0.05$ *v.s.* control.

last restraint exposure, an increase in anxiety-related behavior was found in stressed OTR KO mice compared with the un-stressed KO mice (Fig. 4A). RGS2 levels did not differ between stressed and un-stressed OTR KO females (Fig. 4B).

3. Discussion

The present study provided the following four important findings (Table 2). First, OT induced RGS2 expression in the CeA of female mice. Second, repeated restraint stress also induced RGS2 expression in the CeA. Third, RGS2 levels in the CeA correlated with anxiolysis. Fourth, restraint stress neither increased RGS2 levels in the CeA nor had an anxiolytic effect in OT receptor-deficient or OT receptor antagonist-injected mice.

Psycho-social or physical stressors like restraint stress and forced swimming evoke the release of OT in various areas of the CNS including the amygdala (Ebner et al., 2000; Ebner et al., 2005; Wigger and Neumann, 2002). The release of OT is believed to protect against stress-evoked anxiety. The present study also showed that short-term restraint stress had an

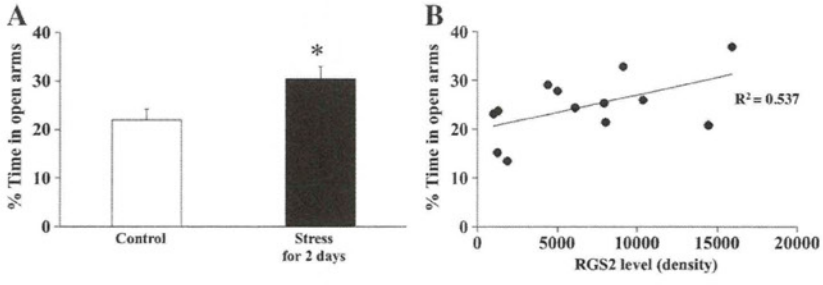

Fig. 3 – Anxiolytic effect of short-term restraint stress. (A) Effect of restraint stress for 2 days on time spent in the open arms on day 3. n = 10 each. * $P < 0.05$ *v.s.* control. (B) Comparison of the Spearman rank correlation between RGS2 levels in the CeA of females and time spent in the open arms. Mice were subjected to restraint stress (4 h/day) for 2 days and then tested on an elevated plus maze on day 3. After the test, mice were sacrificed and the CeA was used for Western blotting of RGS2.

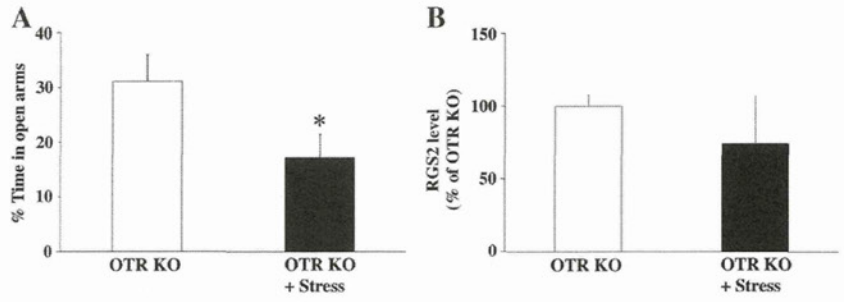

Fig. 4 – Effect of restraint stress on the anxiety of OTR KO mice (A) and RGS2 levels in the CeA (B). (A) OTR KO females were subjected to restraint stress (4 h/day) for 2 days and then tested on an elevated plus maze 24 h after the last stress. n = 5 each. * $P < 0.05$ *v.s.* OTR KO mice with no restraint stress (OTR KO). (B) OTR KO females were subjected to restraint stress (4 h/day) for 2 days. Twenty-four hours after the last stress, the CeA was removed and the RGS2 level was examined by Western blotting.

anxiolytic effect in wild-type females but not in OT receptor-deficient or OT receptor antagonist-injected mice. These results suggest that OT is an important modulator of anxiety and of stress-coping circuitries (Fig. 5).

Anxiety disorders represent one of the most common psychiatric conditions in the World and epidemiological studies have indicated that as many as 29% of people will, at some point in their lives, suffer from anxiety disorders (Hawgood and De Leo, 2008). As a means of gaining a better understanding of the risk factors for developing anxiety disorders as well as to tailor individualized treatment options for anxiety, there has recently been a significant effort to investigate the genetic bases for anxiety disorders (Norrholm and Ressler, 2009). RGS2 was identified as a modulator of anxiety in both mice and humans (Cui et al., 2008; Leygraf et al., 2006; Yalcin et al., 2004). RGS2 represents a potential target for pharmacotherapy and compounds, which induce its expression may provide a potential treatment for anxiety disorders. However, no drugs, hormones or cytokines, which induce RGS2 expression in the CNS, especially in the CeA, have yet been identified. In the present study, we showed that OT induced RGS2 expression in the CeA of mice. Although a number of studies have shown a potential anxiolytic effect of OT, the mechanism involved has been unclear (Slattery and Neumann, 2010). Induction of RGS2 expression may be one mechanism behind the anxiolytic effect of OT and OT may be of therapeutic benefit in subsets of patients with anxiety disorders.

In the present study, we showed that OT functions in female mice. The question of whether OT also has an anxiolytic effect through the induction of RGS2 expression in males arises. OT receptors and OT-binding sites are distributed throughout the amygdala, with a particularly high density in its central part in males (Kremarik et al, 1993; Yoshimura et al, 1993). Force swim stress triggers the release of OT in the CeA of male rats (Ebner et al., 2005). Moreover, sexual activity and mating with a receptive female reduce the level of anxiety and increase risk-taking behavior in male rats and the effect is inhibited by the administration of OTR antagonists (Waldherr and Neumann, 2007). These results suggest that OT may induce RGS2 expression in males. Further study is needed to examine the effect of OT in males as a potential therapeutic for the treatment of anxiety disorders.

The present study focused on RGS2 among OT-induced genes. However, brain-derived neurotrophic factor (BDNF) was also an up-regulated gene in primary cultured neurons treated with OT by microarray analysis (Table 1). In rodents, chronic stress decreases the expression of BDNF, which can lead to neuronal atrophy in the hippocampus and other brain structures, while direct hippocampal infusion of BDNF has anxiolytic and antidepressant effects (Berry et al., in press). Blood BDNF levels are decreased in subjects diagnosed with major depressives, antidepressants can revert this neurobiological change (Berry et al., in press; Duman and Monteggia, 2006). These results suggest that OT may also have anxiolytic effects through the induction of BDNF expression. To investigate whether RGS2 is a principal target of the anxiolytic effects of OT, further study is needed to show whether blockade of upregulation of RGS2 in the CeA such as by siRNA techniques enhance stress-induced anxiety.

In conclusion, OT induces RGS2 expression in the CeA of female mice, resulting in an anxiolytic effect.

Table 2 – A summary of the results.

	Wild-type		OTR KO	
	Nursing	Restraint stress	Restrain stress + OTR antagonist	Restraint stress
RGS2	↑	↑	–	–

↑, up-regulation; –, unchanged.

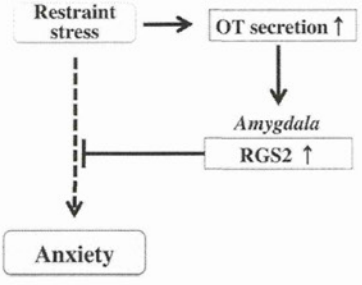

Fig. 5 – Scheme of molecular mechanism on anxiolytic effect of oxytocin.

4. Experimental procedures

4.1. Subjects

Female C57BL6 mice aged 10 to 12 weeks were used for all experiments except those with OT receptor (OTR)-deficient mice.

OTR-deficient mice (OTR-KO) were purchased from Deltagen (San Mateo, CA, USA) (Matsushita et al., 2010). The wild-type (WT) female littermates were used as controls. Originally in an equal mix of the C57BL/6 and 129X1/SvJ strains (RW4 embryonic stem cell line), they have been repetitively backcrossed for 4 generations with C57BL/6 mice (from Deltagen). The females aged 10 to 12 weeks were used for all experiments. The WT females used as controls were littermates.

Animals were housed at 25 °C with 12-h light/dark cycles and free access to water and standard rodent chow in the Department of Animal Resources of Okayama University. To investigate the effect of nursing, pups of female mice were removed immediately after giving birth and their brains were removed 5 days after labor. All procedures were approved by the Animal Ethics Committee of Okayama University (OKU-2010164).

4.2. Application of oxytocin, vasopressin, prolactin and corticotropin-releasing hormone (CRH) in amygdala slices

The brains of virgin mice were quickly removed and immersed in ice-cold artificial cerebrospinal fluid (ACSF) bubbled with a gaseous mixture of 95% O_2 and 5% CO_2. The composition of the ACSF was as follows: NaCl, 124 mM; KCl, 4.4 mM; $CaCl_2$, 2.5 mM; $MgSO_4$, 1.3 mM; NaH_2PO_4, 1 mM; $NaHCO_3$, 26 mM; and glucose, 10 mM. The amygdala region was dissected, and 400-μm transverse slices were prepared using a microtome (VT1200S, Leica Microsystems GmbH, Wetzlar, Germany). The amygdala slices were incubated in ACSF at 30 °C for 1 h before the application of OT. The slices were incubated with 0.1 μM OT (Sigma-Aldrich, St. Louis, MO, USA), 0.1 μM vasopressin (Sigma-Aldrich), 100 ng/ml prolactin (Cedarlane labs, Burlington, Ontario, Canada) or 0.1 μM CRH (Sigma-Aldrich) in a tube for specified periods before protein isolation for Western blotting.

4.3. Microarray analysis

The microarray analysis was performed using a mouse whole genome oligo DNA chip (Agilent Technologies, Santa Clara, CA, USA) as described previously (Fujimura et al, 2011). Briefly, mRNAs (200 ng) from primary cultured neurons treated with 0.1 μM OT or PBS for 2 h and CeA of lactating mice or virgin mice were pooled into separate master total RNA mixes, and labeled with Cy-3 or Cy-5 using an Agilent Low RNA Input Fluorescent Linear Amplification Kit (Agilent Technologies). Hybridization and wash processes were performed according to the manufacturer's instructions, and hybridized microarrays were scanned using an Agilent Microarray scanner G2565BA. For detection of genes with significant differential expression between the control group and mice treated with OT, each image was processed using Agilent Feature Extraction ver.8.5.1.1.

4.4. Western blot analysis

Western blotting was carried out at high stringency, essentially as previously described (Tomizawa et al., 2003). Briefly, the CeA was punched out from amygdala slices. Homogenates of CeA were prepared by sonicating the tissue in boiled 1% SDS buffer. The homogenates (50 μg) were separated by electrophoresis through a 10% SDS-PAGE gel and transferred to a nitrocellulose membrane (GE Healthcare, Uppsala, Sweden). Blots were probed with primary antibodies against RGS2 (1:500 dilution, anti-RGS2 antibody, SC-1020 [Santa Cruz Biotech., Santa Cruz, CA]) and Actin (AC-40, Sigma-Aldrich), and secondary antibodies before the bands were visualized using a commercial ECL detection kit (GE Healthcare). The band densities were normalized to Actin for each sample. The quantitative analysis was performed using analysis software (Quantity One [Bio-Rad, Hercules, CA]).

4.5. Restraint stress

Polypropylene tubes (50-ml conical tubes [Iwaki, Tokyo, Japan]), with holes for proper ventilation, were used to induce restraint stress during the experimental period. Mice were restrained in the tubes for 4 h per day during the dark cycle (1800–2200 h) for the periods indicated.

4.6. Injection of an OT antagonist into the central amygdala

Seven days before the OT injection, mice were placed in a stereotactic device and implanted with an 8-mm long 26-gauge stainless steel cannula just above the left and right CeA (1 mm posterior, 2.5 mm lateral, 1.5 mm ventral from the bregma; Paxinos and Watson). A selective OT receptor (OTR) antagonist, desGly-NH2(9),d(CH2)5[Tyr(Me)2,Thr4] OVT (Sigma-Aldrich), was infused (5 ng/ 0.5 μl) using a 11-mm long 31-gauge needle every 24 h for 5 days (between 9:00 and 10:00). As controls, mice were injected with vehicle (PBS).

Mice were subjected to restraint stress (4 h/day) every 24 h for 4 successive days. The first stress was applied 24 h after the first injection of the OTR antagonist. The time schedule of the experiments is shown in Table 3.

Table 3 – Time schedule of the injection of OT antagonist and restraint stress in mice.

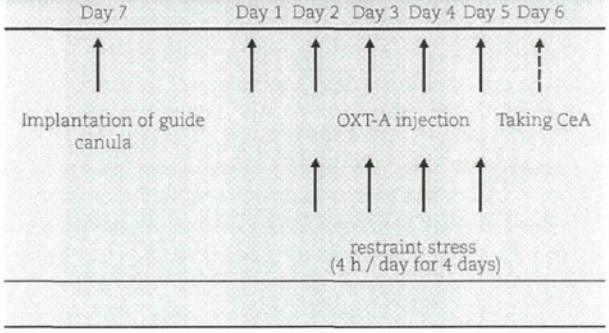

4.7. *Behavioral testing*

Anxiety-related behavior was tested in the elevated plus-maze (EPM), a plus-shaped apparatus elevated above the floor with two dark (7 lux) enclosed arms and two open (30 lux) arms (Lister, 1987). Each mouse was placed in the center of the test apparatus, facing a closed arm, to begin and behavior was monitored with a video camera suspended from the ceiling directly above the center of the maze. Data collection was performed with a digital tracking system (LimeLight ver. 2.0, Actimetrics) interfaced with a Pentium-class personal computer. The time spent in each arm and number of closed and open arm entries were scored for a 5-min test period. Anxiolytic activity was indicated by increased exploration of the open arms of the plus-maze, i.e. by an increased percentage of entries into or percentage of time spent on the open arms of the maze. The total number of entries into closed arms was used as a measure of overall motor activity.

4.8. *Statistics*

Data are shown as the mean ± S.E.M. Student's *t*-test or Mann-Whitney's *U*-test was used to identify significant differences between two conditions and a one-way ANOVA or a two-way ANOVA followed by Tukey-Kramer's *post-hoc* analysis was used to compare multiple conditions. Correlations between each term were analyzed using Pearson's rank correlation coefficient. P values less than 0.05 were considered to be significant.

Acknowledgments

This work was supported by a grant-in-aid for Scientific Research from the Ministry of Education, Culture, Sports, Science and Technology of Japan and by a grant-in-aid for Scientific Research from the Ministry of Health, Labor and Welfare of Japan.

REFERENCES

Argiolas, A., Gessa, G.L., 1991. Central functions of oxytocin. Neurosci. Biobehav. Rev. 15, 217–231.

Bale, T.L., Davis, A.M., Auger, A.P., Dorsa, D.M., McCarthy, M.M., 2001. CNS region-specific oxytocin receptor expression: importance in regulation of anxiety and sex behavior. J. Neurosci. 21, 2546–2552.

Barberis, C., Tribollet, E., 1996. Vasopressin and oxytocin receptors in the central nervous system. Crit. Rev. Neurobiol. 10, 119–154.

Berry, A., Bellisario, V., Capoccia, S., Tirassa, P., Calza, A., Alleva, E., Cirulli, F., in press. Social deprivation stress is a triggering factor for the emergence of anxiety- and depression-like behaviours and leads to reduced brain BDNF levels in C57BL/6 J mice. Psychoneuroendocrinology. doi:10.1016/j.psyneuen.2011.09.007.

Bielsky, I.F., Young, L.J., 2004. Oxytocin, vasopressin, and social recognition in mammals. Peptides 25, 1565–1574.

Blume, A., Bosch, O.J., Miklos, S., Torner, L., Wales, L., Waldherr, M., Neumann, I.D., 2008. Oxytocin reduces anxiety via ERK1/2 activation: local effect within the rat hypothalamic paraventricular nucleus. Eur. J. Neurosci. 27, 1947–1956.

Cui, H., Nishiguchi, N., Ivleva, E., Yanagi, M., Fukutake, M., Nushida, H., Ueno, Y., Kitamura, N., Maeda, K., Shirakawa, O., 2008. Association of RGS2 gene polymorphisms with suicide and increased RGS2 immunoreactivity in the postmortem brain of suicide victims. Neuropsychopharmacology 33, 1537–1544.

Duman, R.S., Monteggia, L.M., 2006. A neurotrophic model for stress-related mood disorders. Biol. Psychiatry 59, 1116–1127.

Ebner, K., Wotjak, C.T., Landgraf, R., Engelmann, M., 2000. A single social defeat experience selectively stimulates the release of oxytocin, but not vasopressin, within the septal brain area of male rats. Brain Res. 872, 87–92.

Ebner, K., Bosch, O.J., Kromer, S.A., Singewald, N., Neumann, I.D., 2005. Release of oxytocin in the rat central amygdala modulates stress-coping behavior and the release of excitatory amino acids. Neuropsychopharmacology 30, 223–230.

Flint, J., 2003. Analysis of quantitative trait loci that influence animal behavior. J. Neurobiol. 54, 46–77.

Fujimura, A., Michiue, H., Nishiki, T., Ohmori, I., Wei, F.Y., Matsui, H., Tomizawa, K., 2011. Expression of a constitutively active calcineurin encoded by an intron- retaining mRNA in follicular keratinocytes. PLoS One 6, e17685.

Gainer, H., Wray, S., 1994. Lactation and its hormonal control. In: Knobil, E., Neill, J.D. (Eds.), The Physiology of Reproduction. Raven, New York, pp. 1099–1129.

Gimpl, G., Fahrenholz, F., 2001. The oxytocin receptor system: structure, function, and regulation. Physiol. Rev. 81, 629–683.

Gray, T.S., 1996. Amygdala: role in autonomic and neuroendocrine responses to stress. In: McCubbin, J.B., Kaufmann, P.G., Nemeroff, C.B. (Eds.), Stress, Neuropeptides and Systemic Disease. Academic Press, San Diego, pp. 37–53.

Han, J.H., Kushner, S.A., Yiu, A.P., Cole, C.J., Matynia, A., Brown, R.A., Neve, R.L., Guzowski, J.F., Silva, A.J., Josselyn, S.A., 2007. Neuronal competition and selection during memory formation. Science 316, 457–460.

Hawgood, J., De Leo, D., 2008. Anxiety disorders and suicidal behavior: an update. Curr. Opin. Psychiatry 21, 51–64.

Heinrichs, M., Baumgartner, T., Kirschbaum, C., Ehlert, U., 2003. Social support and oxytocin interact to suppress cortisol and subjective responses to psychosocial stress. Biol. Psychiat. 54, 1389–1398.

Heximer, S.P., Watson, N., Linder, M.E., Blumer, K.J., Hepler, J.R., 1997. RGS2/G0S8 is a selective inhibitor of Gqα function. Proc. Natl. Acad. Sci. U. S. A. 94, 14389–14393.

Hollinger, S., Hepler, J.R., 2002. Cellular regulation of RGS proteins: modulators and integrators of G protein signaling. Pharmacol. Rev. 54, 527–559.

Hollinger, S., Hepler, J.R., 2004. Methods for measuring RGS protein phosphorylation by H protein-regulated kinases. Methods Mol. Biol. 237, 205–219.

Huber, D., Veinante, P., Stoop, R., 2005. Vasopressin and oxytocin excite distinct neuronal populations in the central amygdala. Science 308, 245–248.

Insel, T.R., Shapiro, L.E., 1992. Oxytocin receptor distribution reflects social organization in monogamous and polygamous voles. Proc. Natl. Acad. Sci. U. S. A. 89, 5981–5985.

Kirsch, P., Esslinger, C., Chen, Q., Mier, D., Lis, S., Siddhanti, S., Gruppe, H., Mattay, V.S., Gallhofer, B., Meyer-Lindenberg, A., 2005. Oxytocin modulates neural circuitry for social cognition and fear in human. J. Neurosci. 25, 11489–11493.

Kosfeld, M., Heinrichs, M., Zak, P.J., Fischbacher, U., Fehr, E., 2005. Oxytocin increases trust in humans. Nature 435, 673–676.

Kremarik, P., Freund-Mercier, M.J., Stoeckel, M.E., 1993. Histoautoradiographic detection of oxytocin- and vasopressinbinding sites in the telencephalon of the rat. J. Comp. Neurol. 333, 343–359.

Labuschagne, I., Phan, K.L., Wood, A., Angstadt, M., Chua, P., Heinrichs, M., Stout, J.C., Nathan, P.J., 2010. Oxytocin attenuates amygdala reactivity to fear in generalized social anxiety disorder. Neuropsychopharmacology 35, 2403–2413.

Leygraf, A., Hohoff, C., Freitag, C., 2006. Rgs 2 gene polymorphisms as modulators of anxiety in humans? J. Neural Transm. 113, 1921–1925.

Lister, R.G., 1987. The use of a plus-maze to measure anxiety in the mouse. Psychophamacology (Berl) 92, 180–185.

Lonze, B.E., Riccio, A., Cohen, S., Ginty, D.D., 2002. Apoptosis, axonal growth defects, and degeneration of peripheral neurons in mice lacking CREB. Neuron 34, 371–385.

Matsushita, H., Tomizawa, K., Okimoto, N., Nishiki, T., Ohmori, I., Matsui, H., 2010. Oxytocin mediates the antidepressant effects of mating behavior in male mice. Neurosci. Res. 68, 151–153.

Neumann, I.D., Torner, L., Wigger, A., 2000a. Brain oxytocin: differential inhibition of neuroendocrine stress responses and anxiety-related behavior in virgin, pregnant and lactating rats. Neuroscience 95, 567–575.

Neumann, I.D., Kromer, S.A., Toschi, N., Ebner, K., 2000b. Brain oxytocin inhibits the (re)activity of the hypothalamo-pituitaryadrenal axis in male rats: involvement of hypothalamic and limbic brain regions. Regul. Peptides 96, 31–38.

Neumann, I.D., 2001. Alterations in behavioral and neuroendocrine stress coping strategies in pregnant, parturient and lactating rats. Prog. Brain Res. 133, 143–152.

Neumann, I.D., 2002. Involvement of the brain oxytocin system in stress coping: interactions with the hypothalamo-pituitaryadrenal axis. Prog. Brain Res. 139, 147–162.

Neumann, I.D., 2008. Brain oxytocin: a key regulator of emotional and social behaviours in both females and males. J. Neuroendocrinol. 20, 858–865.

Norrholm, S.D., Ressler, K.J., 2009. Genetics of anxiety and trauma-related disorders. Neuroscience 164, 272–287.

Numan, M., Insel, T.R., 2003. The Neurobiology of Parental Behavior. Springer, New Jersey.

Oliveira-Dos-Santos, A.J., Matsumoto, G., Snow, B.E., Bai, D., Houston, F.P., Whishaw, I.Q., Mariathasan, S., Sasaki, T., Wakeham, A., Ohashi, P.S., Roder, J.C., Barnes, C.A., Siderovski, D.P., Penninger, J.M., 2000. Regulation of T cell activation, anxiety, and male aggression by RGS2. Proc. Natl. Acad. Sci. U. S. A. 97, 12272–12277.

Siderovski, D.P., Hessel, A., Chung, S., Mak, T.W., Tyers, M., 1996. A new family of regulators of G-protein-coupled receptors? Curr. Biol. 6, 211–212.

Slattery, D.A., Neumann, I.D., 2010. Oxytocin and major depressive disorder: experimental and clinical evidence for links to aetiology and possible treatment. Pharmaceuticals 3, 702–724.

Smoller, J.W., Paulus, M.P., Fagerness, J.A., Purcell, S., Yamaki, L.H., Hirshfeld-Becker, D., Biederman, J., Rosenbaum, J.F., Gelernter, J., Stein, M.B., 2008. Influence of RGS2 on anxiety-related temperament, personality, and brain function. Arch. Gen. Psychiatry 65, 298–308.

Sofroniew, M.V., 1983. Vasopressin and oxytocin in the mammalian brain and spinal cord. Trends Neurosci. 6, 467–472.

Tomizawa, K., Iga, N., Lu, Y.F., Moriwaki, A., Matsushita, M., Li, S.T., Miyamoto, O., Itano, T., Matsui, H., 2003. Oxytocin improves long-lasting spatial memory during motherhood through MAP kinase cascade. Nat. Neurosci. 6, 384–390.

van den Burg, E.H., Neumann, I.D., 2011. Bridging the gap between GPCR activation and behaviour: oxytocin and prolactin signalling in the hypothalamus. J. Mol. Neurosci. 43, 200–208.

Waldherr, M., Neumann, I.D., 2007. Centrally released oxytocin mediates mating-induced anxiolysis in male rats. Proc. Natl. Acad. Sci. U. S. A. 104, 16681–16684.

Wigger, A., Neumann, I.D., 2002. Endogenous opioid regulation of stress-induced oxytocin release within the hypothalamic paraventricular nucleus is reversed in late pregnancy: a microdialysis study. Neuroscience 112, 121–129.

Yalcin, B., Willis-Owen, S.A., Fullerton, J., Meesaq, A., Deacon, R.M., Rawlins, J.N., Copley, R.R., Morris, A.P., Flint, J., Mott, R., 2004. Genetic dissection of a behavioral quantitative trait locus shows that Rgs2 modulates anxiety in mice. Nat. Genet. 36, 1197–1202.

Yoshimura, R., Kiyama, H., Kimura, T., Araki, T., Maeno, H., Tanizawa, O., Tohyama, M., 1993. Localization of oxytocin receptor messenger ribonucleic acid in the rat brain. Endocrinology 133, 1239–1246.